

Some implications of lepton flavor violating processes in a supersymmetric Type II seesaw model at TeV scale

Raghavendra Srikanth Hundi

Department of Theoretical Physics,
Indian Association for the Cultivation of Science,
2A & 2B Raja S.C. Mullick Road,
Kolkata - 700 032, India.

E-mail address: tprsh@iacs.res.in

Abstract

We have conceived a supersymmetric Type II seesaw model at TeV scale, which has additional particles consisting of scalar and fermionic triplet Higgses, with masses being around few hundred GeV. In this particular model, we have studied constraints arising on the masses of triplet states from the lepton flavor violating processes such as $\mu \rightarrow 3e$ and $\mu \rightarrow e\gamma$. We then have studied implications of these constraints on other observable quantities such as the muon anomalous magnetic moment. We also have studied the decays of scalar triplet Higgses, through which these fields can be detected at collider experiments like the Large Hadron Collider. We have studied on how the constraints from the lepton flavor violation would effect the decay channels of the scalar triplet Higgses.

1 Introduction

The Standard Model (SM) has been a successful model and the only missing piece of it is the Higgs boson, for which, in the recent experiment at the Large Hadron Collider (LHC) a Higgs-like particle has been discovered [1]. As of now the discovery at the LHC experiment does not imply that it is a Higgs boson of the SM and it could even belong to the physics beyond the SM. On going studies at the LHC would confirm on this in future. As for the physics beyond the SM, several motivations have been given [2]. The important motivations among these are the gauge hierarchy problem, smallness of neutrino masses, existence of dark matter, etc. Although there is a growing belief in the physics beyond the SM, the theoretical models in this category also have to deal with the constraints from the flavor violating processes. For a review on flavor violating processes, see [3]. The SM has been consistent with all the flavor violating processes due to the Glashow-Iliopoulos-Maiani cancellation mechanism, and this cancellation mechanism may not work in the models of physics beyond the SM.

In this work, we have been motivated by the physics beyond the SM [2] and especially from the smallness of neutrino masses [4]. Among the various models for neutrino masses, Type II seesaw mechanism offers a viable option [5]. In this mechanism, the scalar triplet Higgs with hypercharge $Y = 1$ can give Majorana masses to neutrinos, by acquiring a vacuum expectation value (vev) to the neutral component of the scalar triplet Higgs. The masses of scalar triplet Higgses would be $\sim 10^{14}$ GeV which brings down the vev of neutral triplet Higgs to be around 1 eV, and thereby for $\mathcal{O}(1)$ Yukawa couplings the neutrino mass scale $m_\nu \sim 0.1$ eV can be explained. Since the gauge hierarchy problem is another motivation for physics beyond the SM, supersymmetry (SUSY) [6, 7] has been proposed and it is one of the main contenders for new physics. To explore the options among the physics beyond the SM, supersymmetrizing the Type II seesaw mechanism would be worth to do [8]. In the supersymmetrized version of Type II seesaw model, both the scalar and fermionic states of triplet Higgses would have super heavy masses of $\sim 10^{14}$ GeV. A positive thing of having super heavy masses to triplet Higgs states is that the lepton flavor violating (LFV) processes in both the non-SUSY and SUSY versions of Type II seesaw model would be suppressed and will be within the experimental limits. A negative point in these models is that the detection of triplet states at the current accelerator-based experiments, like LHC, is highly unlikely to test these models. For indirect signals of super heavy triplet states, see [9]. Hence, for phenomenological studies at LHC, we consider a specific version of SUSY Type-II seesaw model, where we realize

TeV scale masses for the triplet Higgs states.

In the Type II seesaw model, leptogenesis mechanism can be employed to explain the asymmetry between matter and anti-matter [10]. In the non-SUSY version of Type II seesaw model, the recent indication of the LHC experiment on the existence of Higgs boson [1] can also be accommodated [11], and one can address the same issue in the SUSY version of this model as well [12]. In these models, the triplet Higgs states can induce LFV processes like $\mu \rightarrow 3e$, $\tau \rightarrow 3\mu$, $\tau \rightarrow e2\mu$, etc at tree level, and at 1-loop level decays like $\mu \rightarrow e\gamma$, $\tau \rightarrow e\gamma$ and $\tau \rightarrow \mu\gamma$ can also happen. None of the above mentioned LFV decay processes have been observed in experiments and stringent experimental upper bounds have been put on the decay branching ratios of these processes [13]. In the literature, some work has already been done on the LFV processes in the non-SUSY version of Type II seesaw model at TeV scale [14, 15, 16]. Even in the SUSY version of Type II seesaw model at TeV scale, some work has been done in this direction [17]. However, in Ref. [17], a detailed study of constraints on the triplet Higgs states from the LFV processes has not been done. Moreover, in Ref. [17], the model has been motivated from high scale physics, and due to running of parameters with energy scale, the off-diagonal elements in the charged slepton and sneutrino mass matrices at low energy scale can also contribute to the $\mu \rightarrow e\gamma$.

In this work, we have confined to the TeV scale SUSY version of Type II seesaw model at the low energy scale and assume diagonal elements of charged slepton and sneutrino mass matrices. More precisely, we assume off-diagonal elements to be zero in the soft mass-squared terms and also in the soft A -terms of the slepton fields. Hence, in our considered model, the LFV processes can happen only due to the non-diagonal Yukawa couplings of triplet Higgs field to the lepton doublets. By scanning the parametric space in order to be consistent with the above mentioned LFV processes, we have obtained lower bounds on the masses of scalar as well as fermionic states of triplet Higgses. In our scanning analysis, we have found that the lower mass bounds on the scalar states are higher than that of the fermionic states. Next, we have studied the implications of the constraints from the LFV processes on other observable quantities such as the anomalous magnetic moment of the muon [18] and the decays of triplet Higgses. Since the triplet states have TeV scale masses, they can be pair produced at the LHC and their decay products give us experimental signals of this model. We have particularly studied decay branching ratios of scalar triplet Higgses and have pointed out how the constraints from the LFV processes effect the detection channels of these fields.

The organization of our paper is as follows. In the next section, we give a brief

description of SUSY version of Type-II seesaw model at TeV scale. In Sec. 3, we describe various LFV processes and their branching ratios of this model. In Sec. 4, we have presented constraints due to the LFV processes on the masses of scalar and fermionic components of triplet Higgses of the model. In the same section, we have also given results on the contribution of triplet states to the anomalous magnetic moment of the muon, $(g-2)_\mu$. In Sec. 5, we have described various decay channels and their branching ratios of the scalar triplet Higgses. We conclude in Sec. 6. We have given total scalar potential of this model and conventions of neutralino and chargino mass matrices in the Appendix.

2 The Model

The gauge symmetry of the SUSY Type-II seesaw model is $SU(3)_C \times SU(2)_L \times U(1)_Y$ and the superpotential of this model can be written as [8]

$$\begin{aligned} W &= W_{\text{MSSM}} + W_{\text{II}}, \\ W_{\text{MSSM}} &= Y_u^{jk} Q_j H_u D_k^c + Y_d^{jk} Q_j H_d D_k^c + Y_e^{jk} L_j H_d E_k^c + \mu H_u H_d, \\ W_{\text{II}} &= Y_\nu^{jk} L_j i\sigma_2 T_1 L_k + \lambda_1 H_d i\sigma_2 T_1 H_d + \lambda_2 H_u i\sigma_2 T_2 H_u + M \text{Tr}(T_1 T_2). \end{aligned} \quad (1)$$

Here, $j, k = 1, 2, 3$ are the family indices and σ_j are Pauli matrices. Q and L are the quark and lepton $SU(2)_L$ doublet superfields, U^c , D^c and E^c are $SU(2)_L$ singlet superfields which represent up-type, down-type quarks and charged lepton, respectively. H_u and H_d are the $SU(2)_L$ doublet superfields with hypercharges $Y = \frac{1}{2}$ and $-\frac{1}{2}$, respectively. μ and M are the only two mass parameters in the above equation. T_1 and T_2 are the $SU(2)_L$ triplet superfields with hypercharges $Y = 1$ and -1 , respectively. The forms of T_1 and T_2 are as given below.

$$T_1 = \begin{pmatrix} \frac{1}{\sqrt{2}} T_1^+ & T_1^{++} \\ T_1^0 & -\frac{1}{\sqrt{2}} T_1^+ \end{pmatrix}, \quad T_2 = \begin{pmatrix} \frac{1}{\sqrt{2}} T_2^- & T_2^0 \\ T_2^{--} & -\frac{1}{\sqrt{2}} T_2^- \end{pmatrix}. \quad (2)$$

The neutral part of scalar triplet Higgs T_1 can acquire vev, which generates masses to neutrinos, which are given below.

$$M_\nu^{jk} = 2Y_\nu^{jk} v'_1, \quad (3)$$

where $\langle \phi_1^0 \rangle = v'_1$. The factor 2 in the above equation is due to the Majorana nature of neutrino fields. The vev of the neutral scalar part of the T_2 is $\langle \phi_2^0 \rangle = v'_2$, and from

naturalness of parameters we expect $v'_1 \sim v'_2$. Here, we use the convention that the scalar parts of triplet Higgs T_1 are denoted by ϕ_{1s} and their supersymmetric counter parts are denoted by Δ_{1s} . Similar convention applies to T_2 . To generate realistic neutrino masses, we can choose $Y_\nu \sim \mathcal{O}(1)$ and $v'_1 \sim 1$ eV. This choice of vev satisfies the upper limit (~ 1 GeV) on the vev of scalar triplet Higgs, which arises from precision electroweak tests. The Yukawa couplings can be uniquely determined in terms of neutrino mass eigenvalues and mixing angles, whose relation is given below.

$$Y_\nu = \frac{1}{2v'_1} U_{\text{PMNS}}^* M_{\text{diag}} U_{\text{PMNS}}^\dagger, \quad M_{\text{diag}} = \text{diag}(m_1, m_2, m_3), \quad (4)$$

where $m_{1,2,3}$ are the three neutrino mass eigenvalues and U_{PMNS} is the Pontecorvo-Maki-Nakagawa-Sakata unitary matrix. In the actual numerical analysis, we would see that either in the normal or inverted hierarchical pattern of neutrino masses the Yukawa couplings are $Y_\nu \sim 10^{-2}$ for $v'_1 \sim 1$ eV. Unless there is a mechanism to justify the order 2 suppression in Y_ν , we may take this as a natural value in the Type II seesaw mechanism.

In the non-SUSY version of Type II seesaw model, the vev of the neutral component of scalar triplet Higgs arises due to the tri-linear coupling of its to the doublet Higgs [14, 15]. In the SUSY version of Type II seesaw model, these tri-linear couplings are equivalent to the $\lambda_{1,2}$ -terms of Eq. (1). To realize the possibility of $v'_{1,2} \sim 1$ eV, we can take the dimensionless parameters $\lambda_{1,2} \sim \mathcal{O}(1)$ and the supersymmetric triplet Higgs mass $M \sim 10^{14}$ GeV [8]. However, as explained before, in this case the masses of scalar and fermionic components of triplet Higgs would be super heavy and direct search for them at colliders is unlikely. Alternatively, we can consider another possibility where $\lambda_{1,2} \sim 10^{-10}$ and $M \sim 1$ TeV [17]. In this later case, components of triplet Higgses would be accessible at the on-going LHC experiment. The justification for the suppression of dimensionless couplings can be given if we embed the model in a high scale theory like supergravity [17]. Supergravity is a realistic scenario where supersymmetry breaking can be achieved through some gauge singlet fields known as hidden sector fields (X) [6, 7]. Hidden sector fields can break supersymmetry at an intermediate energy scale $\langle X \rangle = \Lambda \sim 10^{11}$ GeV, and as a result, the supersymmetric fields would have a mass of about $\frac{\Lambda^2}{M_P} \sim 1$ TeV. Here, M_P is the Planck scale which is $\sim 10^{19}$ GeV. By embedding the model in a high scale theory, we may identify $\lambda_{1,2} \sim Y_\nu \frac{\langle X \rangle}{M_P}$, which gives the necessary suppression in the $\lambda_{1,2}$. Although a realistic construction of the above model can be made by embedding it in a high scale theory ¹, it is beyond the scope of this work. We here, on the phenomenological grounds, consider a low energy setup of the above described SUSY Type II seesaw model,

¹See [19], for embedding of another variety of SUSY model in a supergravity setup.

in which we assume suppressed values of $\lambda_{1,2}$ so that we can choose the supersymmetric masses of this model to be around 1 TeV.

The implication of supersymmetry breaking is to generate soft terms in the low energy regime of the scalar potential. See Appendix A for a general form of the scalar potential in this model. Apart from the soft terms of minimal SUSY SM (MSSM) [6, 7], the terms containing the triplet Higgses can be written as follows.

$$V_{\text{soft}}^{\text{triplet}} = m_{\phi_1}^2 \text{Tr}(\Phi_1^\dagger \Phi_1) + m_{\phi_2}^2 \text{Tr}(\Phi_2^\dagger \Phi_2) + [B_T M \text{Tr}(\Phi_1 \Phi_2) + (A_\nu Y_\nu)^{jk} \tilde{L}_j i \sigma_2 \Phi_1 \tilde{L}_k + (A_{\lambda_1} \lambda_1) H_d i \sigma_2 \Phi_1 H_d + (A_{\lambda_2} \lambda_2) H_u i \sigma_2 \Phi_2 H_u + \text{h.c.}], \quad (5)$$

where the form of $\Phi_{1,2}$ is same as that of $T_{1,2}$ with its superfields being replaced by their scalar components. All the various mass parameters in the above equation would be at around 1 TeV. The term $\text{Tr}(\Phi_1 \Phi_2)$ gives mixing masses between components of Φ_1 and Φ_2 . In the following basis: $\psi_{++} = (\phi_1^{++}, (\phi_2^{--})^*)^T$, $\psi_+ = (\phi_1^+, (\phi_2^-)^*)^T$, $\psi_0 = (\phi_1^0, (\phi_2^0)^*)^T$, the mixing mass-squared matrices are as given below.

$$\psi_{++}^\dagger M_{++}^2 \psi_{++}, \quad \psi_+^\dagger M_+^2 \psi_+, \quad \psi_0^\dagger M_0^2 \psi_0. \quad (6)$$

The form of M_{++}^2 is

$$M_{++}^2 = \begin{pmatrix} M^2 + m_{\phi_1}^2 + m_{++}^2 & (B_T M)^* \\ B_T M & M^2 + m_{\phi_2}^2 - m_{++}^2 \end{pmatrix}, \quad (7)$$

where $m_{++}^2 = \frac{g^2 - g'^2}{2} \cos(2\beta) v^2$, which arises due to the electroweak correction to the doubly charged scalar ϕ -fields, which in turn happen due to D -terms in the SUSY scalar potential, see Appendix A. The forms of M_+^2 and M_0^2 are same as that of M_{++}^2 , except that replace m_{++}^2 by $m_+^2 = -\frac{g'^2}{2} \cos(2\beta) v^2$ and $m_0^2 = -\frac{g^2 + g'^2}{2} \cos(2\beta) v^2$ in the M_+^2 and M_0^2 , respectively. Here, we have taken the electroweak scale as $v = 174$ GeV and β is defined as $\tan \beta = \langle H_u^0 \rangle / \langle H_d^0 \rangle$, which is the ratio of vevs of up- and down-type doublet Higgses. g, g' are the gauge couplings of $\text{SU}(2)_L$ and $\text{U}(1)_Y$ gauge groups, respectively. Since the above mixing mass matrices (M_{++}^2, M_+^2, M_0^2) are hermitian, they can be diagonalized by the unitary matrices which we denote by U^{++}, U^+ and U^0 , respectively.

Before concluding this section, we comment on the masses of fermionic components of the triplet Higgses. From the last term of W_{II} , Eq. (1), dominant contribution to the masses of these fields is M . However, after electroweak symmetry breaking, fermionic fields like Δ_1^+, Δ_2^- and $\Delta_{1,2}^0$ will have some mixing masses with Higgsinos, winos and bino. Because of this mixing, the 4×4 neutralino mixing mass matrix [6, 7] of MSSM will be

extended to 6×6 , and similarly the chargino mass matrix [6, 7] will be extended to 3×3 in this model. The mixing masses can happen due to $\lambda_{1,2}$ terms of W_{II} and also due to gauge invariant kinetic D -terms of $T_{1,2}$ (See Sec. 5 for D -terms of T_1 and D -terms of T_2 can be analogously written). The corrections due to former terms are negligible due to the suppressed values of $\lambda_{1,2}$. The later terms also give negligible corrections because these mixing masses are proportional to the vevs of scalar triplet Higgses. Since these corrections are ~ 1 eV, we can safely take all the fermionic states of triplet Higgses to be degenerate with a mass of M . Since the mixing with triplet fermionic states are very small, in this work, we have taken both the neutralino and chargino mass matrices to be 4×4 and 2×2 , respectively, which are described in Appendix B.

3 LFV processes

As described in Sec. 1, in our model, we assume vanishingly small off-diagonal elements in the soft mass-squared and A -terms of the charged slepton and sneutrino fields. As a result of this, in the lepton sector of our model, the off-diagonal elements of the first term of W_{II} , Eq. (1), can only generate flavor changing processes, whose interaction terms in the Lagrangian are given below.

$$\mathcal{L} = Y_{\nu}^{jk} \left[-2\nu_L^j \Delta_1^0 \tilde{\nu}_L^k - \nu_L^j \nu_L^k \phi_1^0 + \sqrt{2} (\nu_L^j \Delta_1^+ \tilde{e}_L^k + e_L^j \Delta_1^+ \tilde{\nu}_L^k + \nu_L^j e_L^k \phi_1^+) + 2e_L^j \Delta_1^{++} \tilde{e}_L^k + e_L^j e_L^k \phi_1^{++} \right] + \text{h.c.} \quad (8)$$

The last term of the above equation generate LFV processes at tree level such as $\mu^- \rightarrow e^+ e^- e^-$, $\tau^- \rightarrow e^+ e^- e^-$, $\tau^- \rightarrow \mu^+ e^- \mu^-$, $\tau^- \rightarrow e^+ \mu^- \mu^-$, $\tau^- \rightarrow e^+ e^- \mu^-$, $\tau^- \rightarrow \mu^+ e^- e^-$, $\tau^- \rightarrow \mu^+ \mu^- \mu^-$. The upper limit on the branching ratio of $\mu^- \rightarrow e^+ e^- e^-$ is 10^{-12} [13], whereas, for the remaining decays of τ the upper bound on their branching ratios are about $\sim 10^{-8}$ [13]. These LFV processes are driven by the scalar field ϕ_1^{++} . As explained in the previous section that in this model there is a mixing between ϕ_1^{++} and ϕ_2^{--} and hence the contributions due to both these fields should be summed in the decay widths of these processes. Below we have given expressions of the branching ratios of the above mentioned decays.

$$\begin{aligned} BR(\mu^- \rightarrow e^+ e^- e^-) &= \frac{8|Y_{\nu}^{12}|^2 |Y_{\nu}^{11}|^2}{g^4} m_W^4 \left[\frac{|U_{11}^{++}|^2}{m_{\phi_1^{++}}^2} + \frac{|U_{12}^{++}|^2}{m_{\phi_2^{++}}^2} \right]^2, \\ BR(\tau^- \rightarrow \ell_j^+ \ell_m^- \ell_l^-) &= S \frac{16|Y_{\nu}^{j3}|^2 |Y_{\nu}^{lm}|^2}{g^4} m_W^4 \left[\frac{|U_{11}^{++}|^2}{m_{\phi_1^{++}}^2} + \frac{|U_{12}^{++}|^2}{m_{\phi_2^{++}}^2} \right]^2 BR(\tau^- \rightarrow \mu \bar{\nu}_{\mu} \nu_{\tau}), \end{aligned} \quad (9)$$

where m_W , $m_{\phi_{1,2}^{++}}$ are the masses of W -boson and doubly charged ϕ -fields, respectively. Here, $\ell_1 = e$ and $\ell_2 = \mu$ (It should not be confused with our notation of the muon field with the μ -parameter of Eq. (1)). S is a symmetric factor which equals to $\frac{1}{2}$ if $l = m$, otherwise it equals to 1. The branching ratio of $\tau^- \rightarrow \mu \bar{\nu}_\mu \nu_\tau$ is ≈ 0.17 . As explained previously that the values of Yukawa couplings are determined from the neutrino mass eigenvalues and mixing angles, hence the above described upper limits on the LFV processes would put a lower limit on the masses of doubly charged scalar fields. As explained before that due to similarity in the matrices M_{++}^2, M_+^2, M_0^2 , the above bounds on the doubly charged field will translate into similar lower bounds on the singly charged and neutral scalar triplet fields. Hence, we can conclude that the above mentioned LFV processes can constraint the masses of scalar components of the triplet states, if not of their supersymmetric counterparts. We can gain some in-sight into the masses of fermionic triplet Higgses from the loop induced LFV processes such as $\mu \rightarrow e\gamma$, $\tau \rightarrow e\gamma$ and $\tau \rightarrow \mu\gamma$. The experimental branching ratio of $\mu \rightarrow e\gamma$ is found to be less than 2.4×10^{-12} at 90% C.L. [20], and the corresponding branching ratios of the decays $\tau \rightarrow e\gamma$ and $\tau \rightarrow \mu\gamma$ should be less than about 10^{-8} [13]. We will show later that the upper bounds on the branching ratios of radiative LFV processes can put lower bounds on the masses of fermionic triplet Higgses.

Let us consider the decay process $\ell_j(p) \rightarrow \ell_i(p') + \gamma(q)$, which takes place at one loop level. Here, $i, j = 1, 2, 3$ are family indices. ℓ_i and ℓ_j are some negatively charged leptons with 4-momenta p' and p , respectively. The outgoing γ has 4-momenta $q = p - p'$. In this model, the 1-loop decay $\ell_j \rightarrow \ell_i + \gamma$ is driven by virtual exchanges of $\phi_1^{++} - \ell$, $\phi_1^+ - \nu$, $\Delta_1^{++} - \tilde{l}$ and $\Delta_1^+ - \tilde{\nu}$. Here, $\tilde{l}, \tilde{\nu}$ are charged slepton and sneutrino fields, respectively. In the below calculation we have neglected the left-right mixing in the charged sleptons, which is proportional to the masses of the corresponding charged leptons. The decay width of the above process is governed by the amplitude which has the following form, where there is no summation on the indices i, j .

$$i\mathcal{M} = ie\bar{u}_i(p') \left[A_R^{ij} \frac{1 + \gamma_5}{2} + A_L^{ij} \frac{1 - \gamma_5}{2} \right] i\sigma^{\mu\nu} q_\nu \epsilon_\mu^*(q) u_j(p). \quad (10)$$

Here, u_i and u_j are the Dirac spinors of the charge leptons ℓ_i and ℓ_j , respectively, and $\epsilon_\mu(q)$ is the polarization of photon. The forms of A_R^{ij} and A_L^{ij} are as given below, where

there is no summation on the indices i, j .

$$\begin{aligned}
A_R^{ij} &= A_{ij} m_{\ell_j}, \quad A_L^{ij} = A_{ij} m_{\ell_i}, \\
A_{ij} &= \sum_{k=1}^3 \left\{ -\frac{(Y_\nu^{ki})^* Y_\nu^{kj}}{12\pi^2} \left[\left(\frac{|U_{11}^{++}|^2}{m_{\phi_1^{++}}^2} + \frac{|U_{12}^{++}|^2}{m_{\phi_2^{++}}^2} \right) + \frac{1}{8} \left(\frac{|U_{11}^+|^2}{m_{\phi_1^+}^2} + \frac{|U_{12}^+|^2}{m_{\phi_2^+}^2} \right) \right] \right. \\
&\quad \left. + \frac{(Y_\nu^{ki})^* Y_\nu^{kj}}{16\pi^2 M^2} [2f_1(x_k^{++}) + 4f_2(x_k^{++}) + f_2(x_k^+)] \right\}, \tag{11}
\end{aligned}$$

$$\begin{aligned}
x_k^{++} &= \frac{m_{\tilde{l}_k}^2}{M^2}, \quad x_k^+ = \frac{m_{\tilde{\nu}_k}^2}{M^2}, \\
f_1(x) &= \frac{1}{(1-x)^4} \left[\frac{1}{3} + \frac{x}{2} - x^2 + \frac{x^3}{6} + x \log(x) \right], \\
f_2(x) &= \frac{1}{(1-x)^4} \left[\frac{1}{6} - x + \frac{x^2}{2} + \frac{x^3}{3} - x^2 \log(x) \right]. \tag{12}
\end{aligned}$$

Here, m_{ℓ_i} , $m_{\tilde{l}_k}$ and $m_{\tilde{\nu}_k}$ are the masses of charged lepton, charged slepton and sneutrino fields, respectively. The decay width of $\mu \rightarrow e\gamma$ is given by

$$\Gamma(\mu \rightarrow e\gamma) = \frac{e^2}{16\pi} (|A_R^{12}|^2 + |A_L^{12}|^2) \frac{(m_\mu^2 - m_e^2)^3}{m_\mu^3} \tag{13}$$

After neglecting the electron mass, the branching ratio of $\mu \rightarrow e\gamma$ is

$$Br(\mu \rightarrow e\gamma) = \frac{\Gamma(\mu \rightarrow e\gamma)}{\Gamma(\mu \rightarrow e\bar{\nu}_e\nu_\mu)} = \frac{48\alpha\pi^3}{G_F^2} (A_{12})^2, \tag{14}$$

where $\alpha = \frac{e^2}{4\pi}$ and $G_F = 1.166 \times 10^{-5} \text{ GeV}^{-2}$. The branching ratio of $\tau \rightarrow e\gamma$ can be calculated as

$$Br(\tau \rightarrow e\gamma) = \frac{48\alpha\pi^3}{G_F^2} (A_{13})^2 Br(\tau \rightarrow \mu\bar{\nu}_\mu\nu_\tau). \tag{15}$$

In the above expression by replacing $A_{13} \rightarrow A_{23}$, we can get expression for the branching ratio of $\tau \rightarrow \mu\gamma$. In these expressions, we have applied the approximation $m_\mu^2 \ll m_\tau^2$.

The expression for the anomalous magnetic moment of the muon, $(g-2)_\mu$ [18], can be found from the same amplitude of $\ell_j \rightarrow \ell_i + \gamma$, which is described above. By identifying $\ell_i = \ell_j = \mu$, the necessary amplitude for the $(g-2)_\mu$ can be written as follows.

$$i\mathcal{M} = ie\bar{u}_\mu(p') \left[A_R^{22} \frac{1+\gamma_5}{2} + A_L^{22} \frac{1-\gamma_5}{2} \right] i\sigma^{\mu\nu} q_\nu \epsilon_\mu^*(q) u_\mu(p), \tag{16}$$

where u_μ is the Dirac spinor of the muon. From the above amplitude we can read the contribution to the $(g-2)_\mu$ due to the components of the triplet Higgses as

$$\Delta a_\mu^T = (A_R^{22} + A_L^{22}) 2m_\mu = 2A_{22}m_\mu^2 \tag{17}$$

Here, we comment on our results on the decay branching ratios of flavor changing processes with the previously work done in the non-SUSY [15] and SUSY [17] versions of the Type II seesaw model. The tree level processes like $\mu \rightarrow 3e$, $\tau \rightarrow 3e$ are driven by the scalar triplet field. In the limit $B_T = 0$, the mixing between the fields ϕ_1^{++}, ϕ_2^{--} would be vanishing small and the branching ratios for these processes reduce to the expressions given in the non-SUSY version of the Type II seesaw model [15]. In the radiative decay processes, like $\mu \rightarrow e\gamma$, the general amplitude of these processes get contribution from scalar (1st line of Eq. (11)) as well as from fermionic (2nd line of Eq. (11)) components of triplet Higgs. In the vanishingly small mixing between ϕ_1^{++} and ϕ_2^{--} , the contribution from first line of Eq. (11) reduces to the expression as given in [15], while the fermionic triplet contribution of Eq. (11) has similar form as given in [17], however, the sign proportional to the $f_1(x_k^{++})$ is given with a minus sign in [17].

4 Constraints from the LFV processes

Before explaining the constraints due to LFV processes, we here make brief comments on relaxing constraints from the tree level LFV processes. Among these, we can expect stringent limits from $BR(\mu \rightarrow 3e)$. To suppress limits from $BR(\mu \rightarrow 3e)$, we can fine tune the Yukawa couplings Y_ν^{12}, Y_ν^{11} to be vanishingly small [14, 15, 16]. However, it has been reported in [21] that to achieve $Y_\nu^{12} = 0$, the neutrino mixing angle θ_{13} would be too small to be consistent with the recently measured value of its at the Double Chooz, Daya Bay and RENO experiments [22]. Nevertheless, here our motivation is that we would choose generic values of neutrino masses and mixing angles, and study the bounds on the masses of triplet Higgses.

The six neutrino Yukawa couplings in this model, Eq. (4), are completely determined by the neutrino masses and mixing angles. The mixing angles are incorporated in the unitary matrix U_{PMNS} , and we have parameterized this according to the convention in [13]. Here, without loss of generality, we have chosen the CP violating phase δ and the two Majorana phases to be zero. We have taken the neutrino mass-squared differences as [24]: $m_{\text{solar}}^2 = m_2^2 - m_1^2 = 7.62 \times 10^{-5} \text{ eV}^2$ and $m_{\text{atm}}^2 = m_3^2 - m_1^2 = 2.53(-2.4) \times 10^{-3} \text{ eV}^2$. Here, the term in bracket gives inverted hierarchical mass pattern for neutrinos. To be consistent with the above neutrino mass-squared values, we can choose three different

hierarchical mass patterns for neutrinos, which are described below.

$$\begin{aligned}
&\text{Normal hierarchy (NH)} : m_1 = 0, \quad m_2 = m_{\text{solar}}, \quad m_3 = m_{\text{atm}} \\
&\text{Inverted hierarchy (IH)} : m_3 = 0, \quad m_1 = m_{\text{atm}}, \quad m_2 = \sqrt{m_{\text{solar}}^2 + m_1^2} \\
&\text{Degenerate Neutrinos (DN)} : m_1 = 0.3 \text{ eV}, \quad m_2 = \sqrt{m_{\text{solar}}^2 + m_1^2}, \quad m_3 = \sqrt{m_{\text{atm}}^2 + m_1^2}
\end{aligned} \tag{18}$$

As for the mixing angles, we have taken them as: $\sin \theta_{12} = \frac{1}{\sqrt{3}}$, $\sin \theta_{23} = \frac{1}{\sqrt{2}}$ and $\sin \theta_{13} = 0.1737$. Here, $\theta_{13} = 10^\circ$ and the other two angles are fitted to the tri-bimaximal values [25], and all these values are consistent with the global fitting to the neutrino oscillation data, done in [24].

After determining the Yukawa couplings, $BR(\mu \rightarrow 3e)$ can put limits on the $m_{\phi_1^{++}}$ and $m_{\phi_2^{++}}$. However, in this analysis, we also have to know the values of U_{11}^{++}, U_{12}^{++} . For generic SUSY parametric space, where $B_T M \sim M^2 \sim m_{\phi_{1,2}}^2$, $U_{11}^{++}, U_{12}^{++} \sim \mathcal{O}(1)$. Hence the lower bounds on the $m_{\phi_1^{++}}$ and $m_{\phi_2^{++}}$ would be nearly the same. Alternatively, to simplify this task, we may choose the soft parameters $B_T = 0$ and $m_{\phi_1}^2 \sim m_{\phi_2}^2$. In this case, ϕ_1^{++} and ϕ_2^{--} would be decoupled away from each other and we get lower bound on the $m_{\phi_1^{++}}$ from $BR(\mu \rightarrow 3e)$. From Eq. (7), it can be noticed that for $\tan \beta \sim 10$, the electroweak corrections would be ~ 10 GeV. Hence, the lower bound on $m_{\phi_1^{++}}$ would give nearly the same lower bound on the $m_{\phi_2^{++}}$. In fact, the arguments given below Eq. (7) would suggest that similar amount of lower bounds will apply on the singly charged and neutral triplet scalar fields. Hence, from the above argument of simplicity, we choose $B_T = 0$ in this section.

In Tab. 1 we have presented lower bounds on the mass of ϕ_1^{++} which arises from $BR(\mu \rightarrow 3e) < 10^{-12}$. We have checked that the lower bounds on the $m_{\phi_1^{++}}$ due to

	NH	IH	DN
v'_1	$m_{\phi_1^{++}}$	$m_{\phi_1^{++}}$	$m_{\phi_1^{++}}$
1.0 eV	631.8 GeV	1.71 TeV	1.32 TeV
0.5 eV	1.26 TeV	3.41 TeV	2.64 TeV
0.1 eV	6.32 TeV	17.07 TeV	13.21 TeV

Table 1: Lower bound on the mass of ϕ_1^{++} from $BR(\mu \rightarrow 3e) < 10^{-12}$, for different values v'_1 . These lower bounds are given for all the three hierarchical mass patterns of neutrinos.

$BR(\mu \rightarrow 3e) < 10^{-12}$ would simultaneously satisfy the corresponding experimental upper

bounds on the branching ratios of τ decays such as $\tau \rightarrow 3e$, $\tau \rightarrow e2\mu$, etc. The lower bounds in Tab. 1 can be compared to the lower bound of about 400 GeV on the $m_{\phi^{++}}$ by the CMS collaboration of the LHC experiment [23]. From Tab. 1, we can notice that the lower bounds in the case of NH are much lower compared to that of IH and DN cases. The product $Y_\nu^{12} \times Y_\nu^{11}$, which determines $BR(\mu \rightarrow 3e)$, is lower in the case of NH compared to that of IH and DN cases. However, if we look at numerical values, for $v'_1 = 1.0$ eV, in both the normal and inverted hierarchies, the Yukawa couplings would be around 10^{-3} , whereas, in the case of degenerate neutrinos the diagonal and off-diagonal Yukawa couplings are around 0.1 and 10^{-4} respectively. The lower bounds on $m_{\phi^{++}}$ increases with decreasing value of v'_1 , since from Eq. (4) we see that $Y_\nu \sim \frac{1}{v'_1}$. In fact, from Tab. 1, for $v'_1 = 0.1$ eV, the masses of scalar triplets are so high that there is very less chance of their detection at the current LHC experiment. It is to remind that the lower bounds on $m_{\phi^{++}}$ would apply at a similar amount on other scalar components of triplet Higgses, apart from electroweak corrections.

Now, by inputting the lower bounds of the scalar components of triplet Higgses in the radiative processes like $\mu \rightarrow e\gamma$, we can derive lower bounds on the masses of fermionic components of triplet Higgses. From the expressions of decay branching ratios of $\ell_j \rightarrow \ell_i\gamma$, which are given in the previous section, we can notice that the masses of charged slepton and sneutrino fields would also contribute to these radiative processes. In our numerical results, we vary the masses of charged slepton ($m_{\tilde{l}}$) and sneutrino ($m_{\tilde{\nu}}$) fields, and study the effects due to them. For simplicity, we have chosen degenerate masses for the three charged sleptons and the three sneutrino fields. Regarding the masses of scalar components of triplet Higgses, as explained previously, the electroweak corrections could be at most ~ 10 GeV, and so in our numerical analysis we take $m_{\phi^{++}} \approx m_{\phi_1^+}$. Moreover, in our analysis, we have fixed the values of $m_{\phi^{++}}$ and $m_{\phi_1^+}$ to the lower limits as given in Tab. 1, and we comment below on what may happen if we increase their values from the lower limits. Among the radiative decays, $\mu \rightarrow e\gamma$ would put severe constraints on the parameters, since its branching ratio is $BR(\mu \rightarrow e\gamma) < 10^{-12}$ [20], which is four orders of magnitude less than that on the branching ratios of $\tau \rightarrow e\gamma$ and $\tau \rightarrow \mu\gamma$ [13]. Nevertheless, we have applied constraints from all the above mentioned radiative LFV processes. In the numerical analysis, for some fixed values of charged slepton and sneutrino masses, we first check if the constraints from the $BR(\tau \rightarrow e\gamma)$ and $BR(\tau \rightarrow \mu\gamma)$ are satisfied, then we would compute $BR(\mu \rightarrow e\gamma)$ as a function of the fermionic triplet Higgs mass, M .

In Fig. 1, in the case of normal hierarchical pattern of neutrino masses, we have given constraints on the M from the above mentioned radiative LFV processes. In Fig. 1(a), we

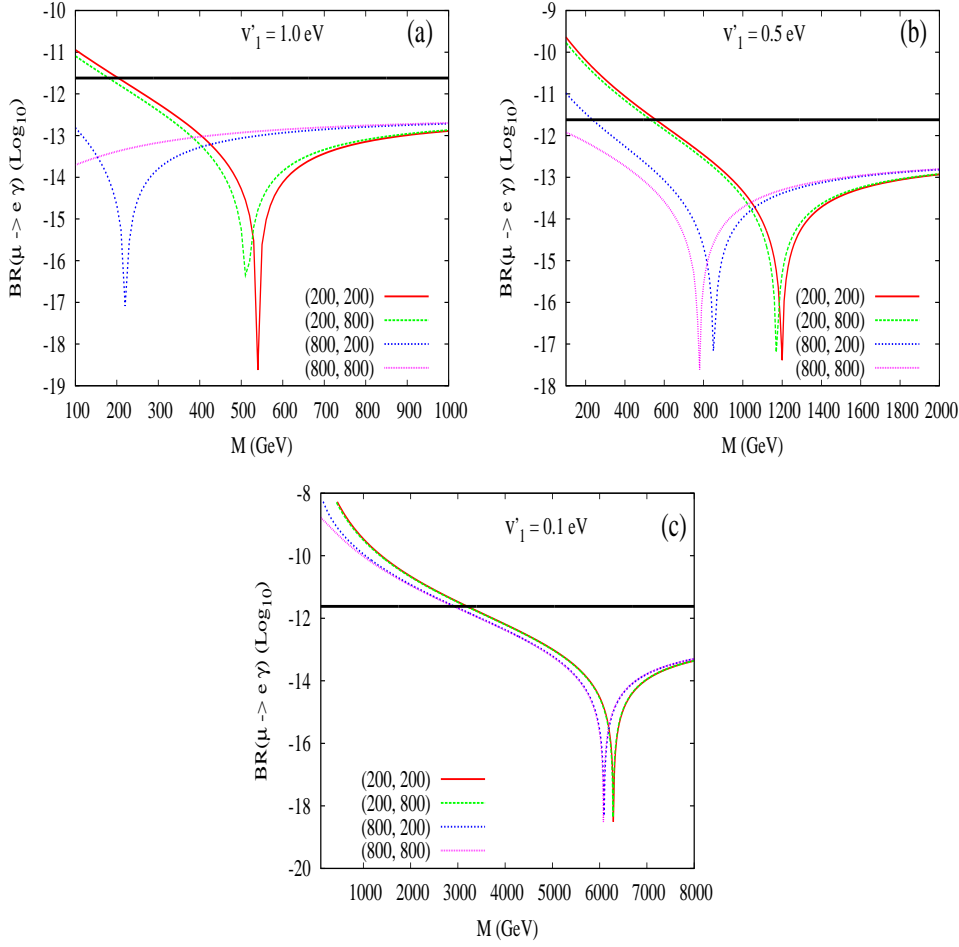


Figure 1: In the normal hierarchy, $Br(\mu \rightarrow e\gamma)$ in the units of \log_{10} , has been plotted against the mass of the fermionic triplet Higgs. The three plots are for $v'_1 = 1.0, 0.5$ and 0.1 eV, which is indicated in the panel. In each of these plots, the four lines are for different values of charged slepton and sneutrino masses, which is represented in the format $(m_{\tilde{l}}, m_{\tilde{\nu}})$ in GeV units. The horizontal line in these plots indicate the current upper limit on $Br(\mu \rightarrow e\gamma)$ at 90% C.L., and the area below this line is allowed. The lower limit on the x-axis is 100 GeV.

have fixed $v'_1 = 1.0$ eV and plotted $BR(\mu \rightarrow e\gamma)$ versus M for four different combinations of $(m_{\tilde{l}}, m_{\tilde{\nu}})$. Among these four different combinations, $(m_{\tilde{l}}, m_{\tilde{\nu}}) = (200 \text{ GeV}, 200 \text{ GeV})$ has given stringent lower limit on the M to be about 200 GeV. The next stringent limit on the M has come from the other combination of $(m_{\tilde{l}}, m_{\tilde{\nu}}) = (200 \text{ GeV}, 800 \text{ GeV})$, which sets $M \geq 180$ GeV. Whereas, the other two combinations such as $(m_{\tilde{l}}, m_{\tilde{\nu}}) = (800 \text{ GeV}, 200 \text{ GeV})$ and $(800 \text{ GeV}, 800 \text{ GeV})$ have put no limits on the M . In Figs. 1(b) and 1(c), we have decreased v'_1 to 0.5 eV and 0.1 eV, respectively. In these two plots we can observe that the lower limits on the M would be stringent from the combination $(m_{\tilde{l}}, m_{\tilde{\nu}}) = (200$

GeV, 200 GeV) compared to the other three combinations that we have mentioned above. The stringent lower limits on the M in Figs. 1(b) and 1(c) are about 550 GeV and 3190 GeV, respectively. From these observations we conclude that the $BR(\mu \rightarrow e\gamma)$ has greater sensitivity on the $m_{\tilde{l}}$ compared to that of $m_{\tilde{\nu}}$, and lower the value of $m_{\tilde{l}}$ the greater would be the lower limit on the M . The lower bounds on the M increases with decreasing v'_1 , since the elements of Yukawa matrix Y_ν would increase. Another point to notice from the plots of Fig. 1 is that the $BR(\mu \rightarrow e\gamma)$ decreases with M and goes to a dip at a certain value of M , and then for a large value of M it becomes saturate. The reason for this is as follows. From the amplitude of the process $\ell_j \rightarrow \ell_i + \gamma$, Eq. (11), we can notice that there is a relative minus sign between the contributions of scalar and fermionic components of the triplet Higgs. Moreover, as explained before, in the numerical analysis, we have fixed the contribution from scalar components by fixing their masses. Hence, due to the above relative minus sign, at a certain value of M the amplitude of $\ell_j \rightarrow \ell_i + \gamma$ would become zero, and then goes to the saturation for large value of M , since the amplitude is $\propto \frac{1}{M^2}$. Since we have fixed the masses of scalar components of triplet Higgs to the lower bounds of Tab. 1, we here comment on what happens if we increase their masses from their lower bounds. Again, due to the above mentioned relative minus sign, we can easily understand that the lower bound on the M increases by increasing the masses of scalar components of triplet Higgs, which we have also noticed numerically. A final comment on the plots of Fig. 1 is that the bounds from the decays $\tau \rightarrow e\gamma$ and $\tau \rightarrow \mu\gamma$ can be seen for $v'_1 = 0.1$ eV but not in the cases of $v'_1 = 1.0$ eV and 0.5 eV. In Fig. 1(c) there are no points for $M < 450$ GeV and $(m_{\tilde{l}}, m_{\tilde{\nu}}) = (200 \text{ GeV}, 200 \text{ GeV})$, because there are not satisfied by the experimental upper limits on the $Br(\tau \rightarrow e\gamma)$ and $Br(\tau \rightarrow \mu\gamma)$. Nevertheless, the constraints from $BR(\mu \rightarrow e\gamma)$ are significant rather than from that of the above mentioned radiative τ decays.

In Figs. 2(a) and 2(b) we have given constraints on the M in the cases of inverted hierarchy and degenerate neutrino mass patterns, respectively. In the cases of both IH and DN, we have noticed that the dependence of $BR(\mu \rightarrow e\gamma)$ on the charged slepton and sneutrino masses is same as that described for Fig. 1. Hence, in both the plots of Fig. 2 we have fixed the masses of charged slepton and sneutrino to a lower value of 200 GeV, which should give stringent limits on the M . We have varied the value of v'_1 in both the plots of Fig. 2. In the case of IH(DN) the lower limit on the M due to $v'_1 = 1.0$ eV, 0.5 eV and 0.1 eV are 210(240) GeV, 570(630) GeV, 3300(3580) GeV, respectively. Comparing these limits with the limits presented in the previous paragraph, the lower bound on the M in the case of IH are intermediate between NH and DN cases, and that the limits in

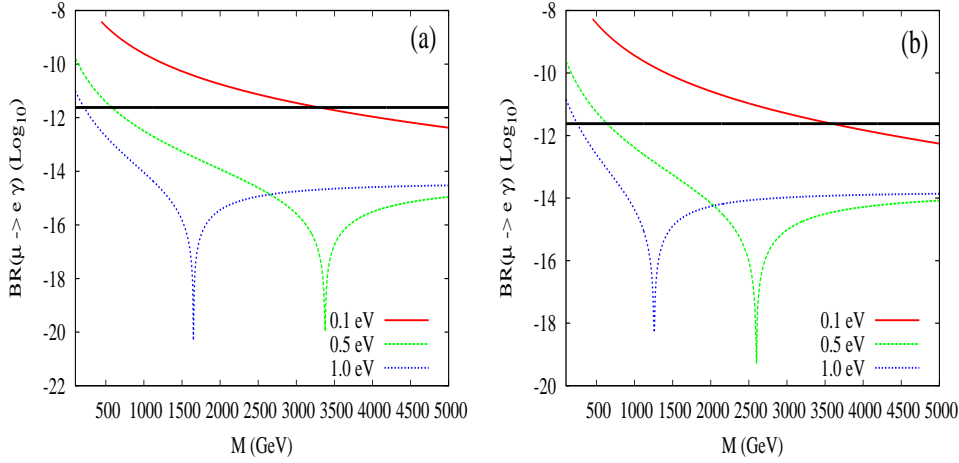


Figure 2: $Br(\mu \rightarrow e\gamma)$ in the units of \log_{10} has been plotted against the mass of the fermionic triplet Higgs. The left plot is for inverted hierarchy and the right plot is for degenerate neutrinos. In both these plots charged slepton and sneutrino masses have been taken to be 200 GeV each. The three lines in each of the above plot are for different values of v'_1 in eV units. The horizontal line in these plots indicate the current upper limit on $Br(\mu \rightarrow e\gamma)$ at 90% C.L., and the area below this line is allowed. The lower limit on the x-axis is 100 GeV.

the DN case are stronger. In both the plots of Fig. 2, we can notice the constraints from $Br(\tau \rightarrow e\gamma)$ and $Br(\tau \rightarrow \mu\gamma)$ in the case of $v'_1 = 0.1$ eV, where points for $M < 450$ GeV are not satisfied by them.

After discussing the limits on the masses of scalar and fermionic components of triplet Higgs from various LFV processes, we now discuss the contribution of these triplet fields to the anomalous magnetic moment of the muon, $(g-2)_\mu$ [18]. The current discrepancy between the SM and the experimental value of the $(g-2)_\mu$ can be taken as $\Delta a_\mu = a_\mu^{\text{EXP}} - a_\mu^{\text{SM}} = (29 \pm 9) \times 10^{-10}$ [18], where $a_\mu = \frac{(g-2)_\mu}{2}$. The $(g-2)_\mu$ is a good observable quantity in the study of new physics. In our model of SUSY Type II seesaw at TeV scale, neutralino–charged slepton and chargino–sneutrino loops would give contribution to the $(g-2)_\mu$ [26], and the above discrepancy can be easily fitted ². On top of the above mentioned loops, the scalar and fermionic components of triplet Higgs would also give some more contribution to the $(g-2)_\mu$, which is given in Eq. (17). From the relation in Eq. (17) we can notice that the contribution from the scalar triplet Higgs states is negative and that from the fermionic triplet Higgses it is positive. Since the current discrepancy in Δa_μ is strictly positive, the non-SUSY Type II seesaw model, where the contribution

²For a recent fit to the $(g-2)_\mu$ in a model similar to the MSSM, see [27].

is from scalar triplet Higgses, cannot explain this discrepancy [16]. Since fermionic triplet Higgses give a positive contribution, it is interesting to see how large the contribution from the components of triplet Higgses to the $(g - 2)_\mu$. The contribution of Δa_μ^T , Eq. (17), greatly depends on the size of the Yukawa couplings. As mentioned before that for $v'_1 = 1.0$ eV, all the Yukawa couplings in the cases of NH and IH would be about 10^{-3} and these couplings would be $\sim 10^{-2}$ for $v'_1 = 0.1$ eV. Since the Yukawa couplings in the cases of NH and IH are so small, we do not expect appreciable amount from the Δa_μ^T . Whereas, in the case of DN, the diagonal and off-diagonal couplings are around 1.5 and $\sim 10^{-3}$, respectively, for $v'_1 = 0.1$ eV. Hence, at least from the diagonal Yukawa coupling Y_ν^{22} we can expect an enhancement to the Δa_μ^T .

In Fig. 3 we have plotted the Δa_μ^T versus M in the case of degenerate neutrino mass pattern. In this figure we have kept the masses of the scalar triplet Higgses to the lower

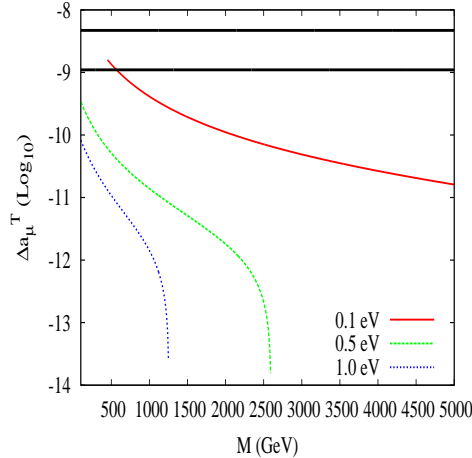


Figure 3: The contribution of triplet Higgses to the $(g - 2)_\mu$, in the units of \log_{10} , has been plotted against M in the case of degenerate neutrinos. The masses of charged slepton and sneutrino have been fixed to 200 GeV each. The three lines in the plot are for different values of v'_1 in the units of eV. The horizontal lines represent the lower and upper end of the 2σ limit of Δa_μ , see text for details.

limit as given in Tab. 1, and also included the constraints from the $\tau \rightarrow e\gamma$ and $\tau \rightarrow \mu\gamma$. The lower and upper horizontal lines in Fig. 3 represent the 2σ limits of the discrepancy in Δa_μ , which can be taken as 1.1×10^{-9} and 4.7×10^{-9} , respectively. The area between these lines is allowed from the $(g - 2)_\mu$. For $v'_1 = 1.0$ eV and 0.5 eV the Yukawa couplings are small that the discrepancy in the $(g - 2)_\mu$ cannot be fitted by the triplet Higgses. Whereas, for $v'_1 = 0.1$ eV there is a chance to fit this discrepancy for a low value of M , however, the constraint from the $\mu \rightarrow e\gamma$ puts a lower limit on M to be around 3600 GeV.

Hence, after including the constraints from the LFV processes the maximum contribution to the $(g-2)_\mu$ from triplet Higgses in this model is found to be 3.4×10^{-11} for $v'_1 = 0.1$ eV, or 0.5 eV, or 1.0 eV. This contribution is two orders smaller than the required amount, and hence the conclusions made above with respect to neutralino-charged slepton and chargino-sneutrino loop contributions to the $(g-2)_\mu$ are unaltered. The discontinuity in the lines of Fig. 3 happen because after certain large value of M , the scalar contribution to the Δa_μ^T would be dominant which is negative and we have plotted Δa_μ^T in the units of \log_{10} . The amount of the negative value is so small that it gives negligible contribution to the $(g-2)_\mu$.

5 Decays of scalar triplet Higgses

Detection of components of triplet Higgses at the LHC experiment gives the validity of our model. At the LHC or an e^+e^- collider, through the γ and Z mediated processes, both the charged as well as the neutral components of triplet Higgses can be pair produced. The production of fermionic components (Δ s) of triplet Higgses is similar to the production of charginos of the MSSM model at the above mentioned colliders. For the production of scalar triplet Higgses at collider experiments, see [28]. Here we study on the decay products of the components of the triplet Higgses, through which the detection of the triplet Higgses would be done at the colliders. In this work we focus on the decays of scalar components of the triplet Higgses. The decays of the fermionic components of triplet Higgses in a left-right SUSY model can be found in [29].

Among the scalar components of the triplet Higgses, decays of ϕ_1^{++} , ϕ_1^+ and ϕ_1^0 are interesting to study, since these states are analogs of the scalar triplet states in the non-SUSY version of Type II seesaw model at TeV scale. As mentioned before that for $B_T \neq 0$ the above mentioned ϕ_1 s will have mixing with the ϕ_2 s, and hence ϕ_2 s can also decay in a similar way as that of ϕ_1 s. Apart from this, from gauge couplings and D -terms in the SUSY scalar potential (see Appendix A), there can also be decays like $\phi_{1,2}^{++} \rightarrow \phi_{2,1}^+ W^+$, $\phi_{1,2}^{++} \rightarrow \phi_{1,2}^+ W^+$, $\phi_{1,2}^{++} \rightarrow \phi_{1,2}^+ H^+$, etc, where H^+ is the charged component of the doublet Higgs boson. Nevertheless, to simplify the many possible decays of scalar triplet Higgses, we choose $B_T = 0$ in our study here, which forbids decays like $\phi_{1,2}^{++} \rightarrow \phi_{2,1}^+ W^+$. After putting the mixing between the ϕ_1 s and ϕ_2 s to be zero, the mass splitting among the doubly charged, singly charged and neutral fields of ϕ_1 and ϕ_2 could be at most ~ 10 GeV for $\tan \beta \sim 10$. As a result of this, decays like $\phi_{1,2}^{++} \rightarrow \phi_{1,2}^+ H^+$, $\phi_{1,2}^{++} \rightarrow \phi_{1,2}^+ W^+$, etc would be kinematically forbidden. After this simplification is done, the ϕ_1 s are exactly similar

to the corresponding scalar triplets in the non-SUSY version of Type II seesaw model, and here we can see the distinction between these two models from the decays of ϕ_1 s.

The scalar ϕ_1 states can decay into charged leptons and neutrinos, for which the interaction terms can be read out from Eq. (8). The components of ϕ_1 can also decay into scalar states involving charged sleptons and sneutrinos. These decays are driven by the $(A_\nu Y_\nu)$ -term of Eq. (5). From the gauge invariant kinetic term of the superfield T_1 , the ϕ_1 s can also decay into supersymmetric fields, whose interaction terms can be obtained from

$$\begin{aligned}\mathcal{L} &= \left(T_1^\dagger e^{2gT^a W^a + 2g'B} T_1\right)_D, \\ &\ni -\sqrt{2}(\phi_1^{++})^* \left[(g\tilde{W}^3 + g'\tilde{B})\Delta_1^{++} + g\tilde{W}^+ \Delta_1^+\right] - \sqrt{2}(\phi_1^+)^* \left[g\tilde{W}^- \Delta_1^{++} + g'\tilde{B}\Delta_1^+ + g\tilde{W}^+ \Delta_1^0\right] \\ &\quad - \sqrt{2}(\phi_1^0)^* \left[g\tilde{W}^- \Delta_1^+ + (-g\tilde{W}^3 + g'\tilde{B})\Delta_1^0\right] + \text{h.c.}\end{aligned}\quad (19)$$

Here, T^a are the generators of the $\text{SU}(2)_L$ group in the triplet representation, which are given in the Appendix A. According to this representation, the form of T_1 in the above equation should be $T_1 = (T_1^{++}, T_1^+, T_1^0)^T$. W^a, B are the gauge superfields of the $\text{SU}(2)_L$ and $\text{U}(1)_Y$ groups, respectively. $\tilde{W}^\pm = \frac{1}{\sqrt{2}}(\tilde{W}^1 \mp i\tilde{W}^2)$. In the above equation, terms involving \tilde{B} and \tilde{W}^3 give interactions with the neutralinos, N_k , $k = 1, \dots, 4$. Similarly, terms involving \tilde{W}^\pm give interactions with the charginos, χ_k^\pm , $k = 1, 2$. Our convention of the neutralino and chargino mass matrices and their diagonalizing unitary matrices are given in Appendix B. In Appendix B, we have taken V^N and V^χ, U^χ as the diagonalizing unitary matrices for neutralinos and charginos, respectively.

The decay widths of ϕ_1 s into leptonic and into SUSY fermionic particles will have the following form.

$$\begin{aligned}\Gamma(\phi_1 \rightarrow AB) &= \frac{1}{8\pi m_{\phi_1}^3} C_{\phi_1, A, B} \sqrt{\lambda(m_{\phi_1}, m_A, m_B)} (m_{\phi_1}^2 - m_A^2 - m_B^2), \\ \lambda(m_{\phi_1}, m_A, m_B) &= m_{\phi_1}^4 + m_A^4 + m_B^4 - 2m_{\phi_1}^2 m_A^2 - 2m_A^2 m_B^2 - 2m_{\phi_1}^2 m_B^2.\end{aligned}\quad (20)$$

Whereas, the decay widths of ϕ_1 s into a pair of scalar states involving charged sleptons or sneutrinos will have the following form.

$$\Gamma(\phi_1 \rightarrow AB) = \frac{1}{16\pi m_{\phi_1}^3} C_{\phi_1, A, B} \sqrt{\lambda(m_{\phi_1}, m_A, m_B)}.\quad (21)$$

Here, A and B are the product particles with masses m_A and m_B , respectively. m_{ϕ_1} is the mass of the parent particle ϕ_1 . In the above Eqs. (20) and (21), the factor $C_{\phi_1, A, B}$ depends on the coupling strength of the parent particle to the product particles, whose values are given in Tab. 2.

$\phi_1 \rightarrow AB$	$C_{\phi_1, A, B}$	$\phi_1 \rightarrow AB$	$C_{\phi_1, A, B}$
$\phi_1^{++} \rightarrow \ell_j^+ \ell_k^+$	$2S Y_\nu^{jk} ^2$	$\phi_1^{++} \rightarrow \tilde{\ell}_j^+ \tilde{\ell}_k^+$	$S (A_\nu Y_\nu)^{jk} ^2$
$\phi_1^{++} \rightarrow \Delta_1^{++} N_k$	$ gV_{2k}^N + g'V_{1k}^N ^2$	$\phi_1^{++} \rightarrow \Delta_1^+ \chi_k^+$	$g^2 V_{1k}^\chi ^2$
$\phi_1^+ \rightarrow \nu_j \ell_k^+$	$ Y_\nu^{jk} ^2$	$\phi_1^+ \rightarrow \tilde{\nu}_j^* \tilde{\ell}_k^+$	$\frac{1}{2} (A_\nu Y_\nu)^{jk} + (A_\nu Y_\nu)^{kj} ^2$
$\phi_1^+ \rightarrow \Delta_1^+ N_k$	$g'^2 V_{1k}^N ^2$	$\phi_1^+ \rightarrow \Delta_1^{++} \chi_k^-$	$g^2 U_{1k}^\chi ^2$
$\phi_1^+ \rightarrow \Delta_1^0 \chi_k^+$	$g^2 V_{1k}^\chi ^2$		
$\phi_1^0 \rightarrow \nu_j \nu_k$	$2S Y_\nu^{jk} ^2$	$\phi_1^0 \rightarrow \tilde{\nu}_j^* \tilde{\nu}_k^*$	$S (A_\nu Y_\nu)^{jk} ^2$
$\phi_1^0 \rightarrow \Delta_1^0 N_k$	$ gV_{2k}^N - g'V_{1k}^N ^2$	$\phi_1^0 \rightarrow \Delta_1^+ \chi_k^-$	$g^2 U_{1k}^\chi ^2$

Table 2: Various decay modes of ϕ_1 s and the factors $C_{\phi_1, A, B}$ which are needed in the Eqs. (20) and (21). In the decay modes into leptons and sleptons, S is a symmetric factor which equals to $\frac{1}{2}$ if $j = k$, otherwise it equals to 1.

In this work we have considered the dominant tree level decays of triplet scalar fields and have neglected loop induced decay processes. At tree level, there can also be additional decays of ϕ_1 s into: (i) di-gauge bosons, (ii) a pair of third family SM fermions, (iii) a pair involving components of doublet Higgses, (iv) gauge boson and a component of doublet Higgs. Some of the representative processes of these additional decays are as follows: $\phi_1^{++} \rightarrow W^+W^+$, $\phi_1^+ \rightarrow t\bar{b}$, $\phi_1^0 \rightarrow H^+H^-$, $\phi_1^+ \rightarrow W^+H^0$. Except the decays in the category of (i), the decays in (ii)–(iv) are driven due to mixing between doublet and triplet scalar Higgses [30]. However, the coupling strengths of all decays in (i)–(iv) are proportional to v'_1 , which in our case is very small, and hence give negligible contribution to branching ratios of these decays. Due to this reasoning, we have neglected the above mentioned decays in our analysis.

The decay widths of ϕ_1 s into SUSY fermionic particles depend on their SUSY masses as well as their coupling strengths, which can be uniquely determined by the following set of parameters: M_1 , M_2 , μ and $\tan \beta$. Here, $M_{1,2}$ are the soft masses of the \tilde{B} and \tilde{W}^a fields, respectively, in the scalar potential. In this work we have chosen these parameters as: $M_1 = 200$ GeV, $M_2 = 300$ GeV, $\mu = 400$ GeV, $\tan \beta = 10$. This set of parameters give neutralino masses as: 195 GeV, 275 GeV, 405 GeV, 434 GeV, and the chargino masses would be 274 GeV and 433 GeV. The above choice of parameters is only for illustration and our conclusions on the branching ratios of ϕ_1 s do not change much with a different set of values. We also have to fix the parameters of $(A_\nu Y_\nu)^{jk}$ which drive the decays of ϕ_1 s into charged sleptons and sneutrinos. For simplicity, we take $(A_\nu Y_\nu)^{jk} = A_\nu (Y_\nu)^{jk}$

and we fix $A_\nu = 500$ GeV. As for the masses of charged sleptons and sneutrinos, we keep their masses to 200 GeV each.

Below we have presented the branching ratios of ϕ_1 s in the case of normal hierarchical mass spectrum of neutrinos. The choice of mass spectrum of neutrinos fix the Yukawa couplings in the decay modes of ϕ_1 s into leptons and sleptons, and this would effect the overall coefficients in the branching ratios. Hence the qualitative features of the branching ratios of ϕ_1 s would be similar in the other cases of inverted hierarchy and degenerate neutrinos.

Decay modes of the scalar field ϕ_1^{++} are as follows: same sign charged dilepton ($\ell_j^+ \ell_k^+$), same sign charged di-slepton ($\tilde{\ell}_j^+ \tilde{\ell}_k^+$), doubly charged fermionic triplet and neutralino ($\Delta^{++} N_k$), singly charged fermionic triplet and chargino ($\Delta^+ \chi_k^+$). The branching ratios of ϕ_1^{++} as function of its mass, in the case of normal hierarchical spectrum of neutrinos, are given in Fig. 4. While plotting the branching ratios, we have summed over the indices

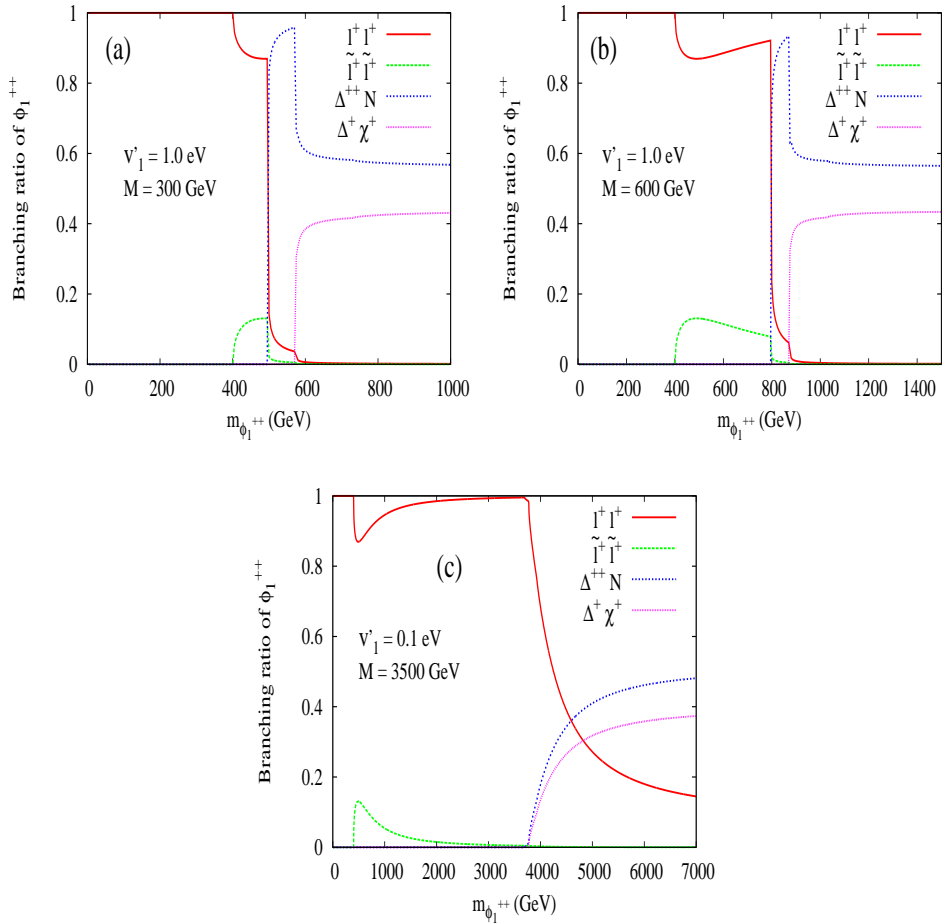


Figure 4: Branching ratios of ϕ_1^{++} decay modes. In all the decay modes we have summed over the generation index of product particles, see text for details.

j, k . For instance, the branching ratio of ϕ_1^{++} into same sign charged dileptons is taken as $Br(\phi_1^{++} \rightarrow \ell^+ \ell^+) = \frac{\sum_{j,k=1}^3 \Gamma(\phi_1^{++} \rightarrow \ell_j^+ \ell_k^+)}{\Gamma_{\phi_1^{++}}}$, where $\Gamma_{\phi_1^{++}}$ is the total decay width of ϕ_1^{++} . Similarly, the three charged sleptons, the four neutralinos and the two charginos are summed in the decay modes of $\phi_1^{++} \rightarrow \tilde{l}^+ \tilde{l}^+$, $\phi_1^{++} \rightarrow \Delta^{++} N$ and $\phi_1^{++} \rightarrow \Delta^+ \chi^+$, respectively. In the plots of Fig. 4, we can notice that both the dilepton and di-slepton modes would be suppressed as soon as the modes into SUSY fermionic particles have opened up. The reason for this is as follows. Apart from coupling strengths, in the limit of large mass of ϕ_1^{++} , the decay widths of ϕ_1^{++} into charged dilepton and into SUSY fermionic particles vary as $\sim m_{\phi_1^{++}}$, while the corresponding decay width of ϕ_1^{++} into charged di-slepton is $\sim \frac{A_\nu^2}{m_{\phi_1^{++}}}$. From the above forms of decay widths, in the limit $m_{\phi_1^{++}} \rightarrow \infty$, it is clear that the decay mode into charged di-slepton cannot stand against modes into SUSY fermionic particles. The decay mode into charged dilepton is driven by Yukawa couplings, which are about $\sim 10^{-3}$ for $v'_1 = 1.0$ eV. Since the decays into SUSY fermionic particles are driven by purely gauge couplings, they would be dominant over the charged dilepton modes as well.

In Fig. 4(a) we have chosen $v'_1 = 1.0$ eV and the mass of fermionic triplet to be 300 GeV, which satisfies the flavor constraints described in the previous section. For $M = 300$ GeV, the SUSY modes involving the neutralinos and charginos would open up at about $m_{\phi_1^{++}} \sim 500$ and 575 GeV, respectively. As argued in the previous section, the LFV processes have put a lower bound on $m_{\phi_1^{++}}$ to be about 630 GeV. Hence, in the case of Fig. 4(a), the scalar field ϕ_1^{++} can be detected at a collider experiment through its decays into SUSY fermionic particles, because both the charged dilepton and charged di-slepton modes are suppressed for $m_{\phi_1^{++}} > 630$ GeV. However, in Fig. 4(b) we have increased M to 600 GeV so that the SUSY fermionic modes would open at about $m_{\phi_1^{++}} \sim 800$ GeV. Now, in this case, there is appreciable branching ratio of $\sim 90\%$ to detect ϕ_1^{++} in the charged dilepton for $m_{\phi_1^{++}}$ between about 630 to 800 GeV. In the same mass range of $m_{\phi_1^{++}} \sim 630\text{--}800$ GeV, the probability of detecting ϕ_1^{++} in the charged di-slepton mode is hardly about 10%. However, by increasing A_ν from 500 GeV to 1 TeV, this probability can be enhanced to 30%, while at the same time the probability into the charged dilepton would decrease to about 70%. In Fig. 4(c) we have decreased v'_1 to 0.1 eV and have taken $M = 3500$ GeV. In this case, there would be enhancement in the Yukawa couplings compared to the previous cases, and the lower limit on $m_{\phi_1^{++}}$ from the LFV processes is about 6300 GeV. Because of the enhancement of the Yukawa couplings, the decay mode into charged dilepton is still significant with a branching ratio of $\sim 17\%$ for $m_{\phi_1^{++}} > 6300$ GeV.

We can compare the results of Fig. 4 with that in the non-SUSY version of Type II seesaw model at TeV scale. In the non-SUSY version, only the decay modes into dilepton and di-gauge boson would be present [30]. However, as argued previously, the decay mode into di-gauge boson would be suppressed in our context. The best channel to detect a scalar triplet Higgs is in the decay $\phi_1^{++} \rightarrow \ell^+ \ell^+$, which has less background in a collider experiment. However, in this model, this channel is restricted by the decay modes into the SUSY particles, and notice how the constraints from the LFV processes are playing a part on the charged dilepton mode. Whereas in the non-SUSY version of Type II seesaw model, even after imposing the constraints from LFV processes, due to non-existence of decay modes into SUSY particles, we would still have high branching ratio for the decay $\phi_1^{++} \rightarrow \ell^+ \ell^+$, provided $v'_1 < 0.1$ MeV [30].

Decay modes of the scalar field ϕ_1^+ are as follows: neutrino and charged lepton ($\nu_j \ell_k^+$), anti-sneutrino and charged slepton ($\tilde{\nu}_j^* \tilde{l}_k^+$), singly charged fermionic triplet and neutralino ($\Delta_1^+ N_k$), doubly charged fermionic triplet and chargino ($\Delta_1^{++} \chi_k^-$), neutral fermionic triplet and chargino ($\Delta_1^0 \chi_k^+$). The branching ratios of ϕ_1^+ as function of its mass are given in Fig. 5, in the case of NH. As explained around Fig. 4, here also, in the branching ratios into

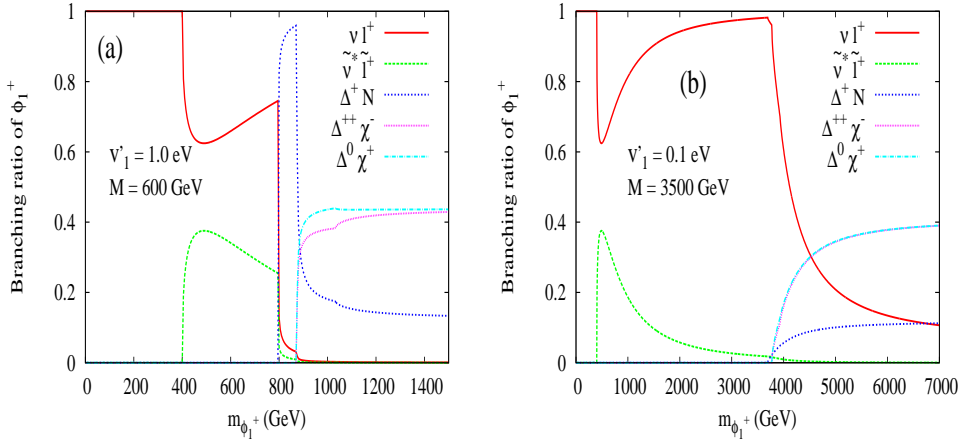


Figure 5: Branching ratios of ϕ_1^+ decay modes. In all the decay modes we have summed over the generation index of product particles, see text for details.

leptons and supersymmetric particles, we have summed over the indices j, k of the leptons, sleptons, neutralinos and charginos. Like what happened in the case of ϕ_1^{++} decays, in Fig. 5 we can observe that the decay modes into leptons and sleptons cannot stand against the modes into SUSY fermionic particles. Unlike in the case of ϕ_1^{++} , the decay $\phi_1^+ \rightarrow \nu \ell^+$ which is driven by Yukawa couplings is not useful for detecting the scalar triplet, since the neutrino is hard to detect in a collider experiment. Hence for detecting the scalar field

ϕ_1^+ , the modes into SUSY fermionic particles are the best ones. The decay channel into $\tilde{\nu}^*$ and \tilde{l}^+ can be used for detection for a certain choice of parametric values. In Fig. 5(a) where $v'_1 = 1.0$ eV and $M = 600$ GeV, the decay channel into $\tilde{\nu}^* \tilde{l}^+$ can be detected in the experiments with a branching ratio of nearly 30% for $m_{\phi_1^+} \sim 630\text{--}800$ GeV. However, as explained around Fig. 4, if we decrease M below about 450 GeV for $v'_1 = 1.0$ eV, the decay channel into $\tilde{\nu}^* \tilde{l}^+$ would be suppressed. In Fig. 5(b) we have put $v'_1 = 0.1$ and $M = 3500$ GeV. In this plot both the decay modes involving chargino particles give approximately the same branching ratio. By comparing the decay modes into SUSY fermionic particles between Figs. 4 and 5, we can notice that for a large value of m_{ϕ_1} the branching ratio of ϕ_1 -decays involving neutralinos have higher percentage compared to that of charginos in Fig. 4, whereas it is vice-versa in Fig. 5. We believe the reason for this is that the coupling of $\phi_1^{++}(\phi_1^+)$ to $\Delta_1^{++}N_k(\Delta_1^+N_k)$ is proportional to $gV_{2k}^N + g'V_{1k}^N(g'V_{1k}^N)$. Since $g > g'$ that would explain the above mentioned observation.

Decay modes of the scalar field ϕ_1^0 are as follows: pair of neutrinos ($\nu_j\nu_k$), pair of anti-sneutrinos ($\tilde{\nu}_j^*\tilde{\nu}_k^*$), neutral fermionic triplet and neutralino ($\Delta_1^0N_k$), singly charged fermionic triplet and chargino ($\Delta_1^+\chi_k^-$). The branching ratios of ϕ_1^0 as function of its mass are given in Fig. 6, in the case of NH. Similar to what we have done in Figs. 4 and 5,

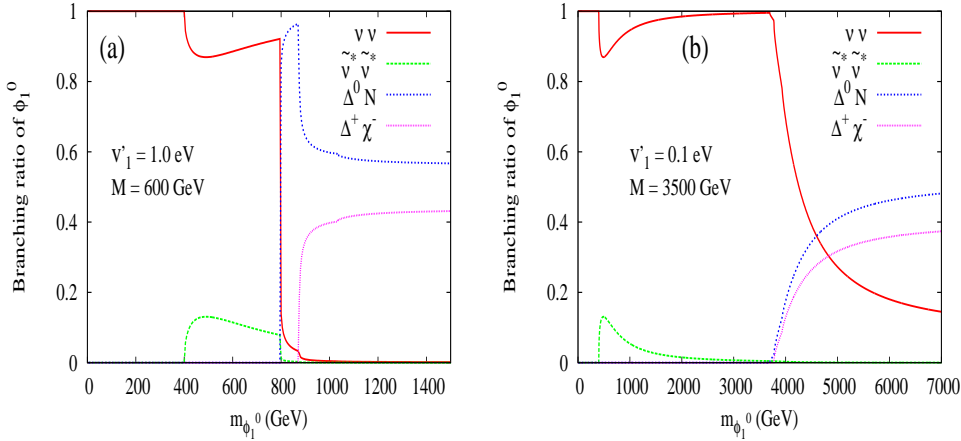


Figure 6: Branching ratios of ϕ_1^0 decay modes. In all the decay modes we have summed over the generation index of product particles, see text for details.

here also we have summed over the indices j, k . Like we have explained for Fig. 5, the detection of ϕ_1^0 can be mainly found from its decays into SUSY fermionic particles, and for some specific choices of v'_1, M we can use the decay channel into a pair of anti-sneutrinos. In Fig. 6(a), the branching ratio for the decay channel into $\tilde{\nu}^* \tilde{\nu}^*$ is not larger than 10% for the allowed region of $m_{\phi_1^0} \sim 630\text{--}800$ GeV. However, this branching ratio can be

increased by increasing the value of A_ν from its input value of 500 GeV here.

A final comment on the decay branching ratios of ϕ_1^+ and ϕ_1^0 , which are described in Figs. 5 and 6, are as follows. In the littlest Higgs model with SU(5) symmetry [31], both the doublet and triplet scalar states of the gauged SU(2)_L would be put into one single SU(5) multiplet. As a result of this, from the Yukawa couplings of top quark, the scalar triplets ϕ^+ and ϕ^0 will have unsuppressed couplings to $t\bar{b}$ and $t\bar{t}$, respectively. Hence, in the littlest Higgs model, the decay branching ratios into $t\bar{b}$ and $t\bar{t}$ give appreciable amount [32]. However, as explained before, in the Type II seesaw model at TeV scale, the above mentioned decay processes are suppressed due to very small admixture between doublet and triplet scalar fields. Hence, in a collider experiment, the decays of singly charged and neutral components of scalar triplet Higgs can be used to distinguish the Type II seesaw model at TeV scale and the littlest Higgs model.

6 Conclusions

In this work we have focused on the phenomenological implications of supersymmetric Type II seesaw model at TeV scale. In this model there are two triplet superfields with hypercharges $Y = +1, -1$, whose scalar and fermionic components will have masses at around TeV scale. We have analyzed a particular framework of this model where LFV processes are driven due to off-diagonal elements of the Yukawa couplings of the triplet field ($Y = +1$) with the lepton doublets. In this framework, LFV processes put constraints on the masses of the components of the triplet Higgses. Specifically, we have found that among the various possible LFV processes, the current experimental upper limits on the branching ratios of $\mu \rightarrow 3e$ and $\mu \rightarrow e\gamma$ can put lower limits on the masses of the scalar and fermionic components of the triplet Higgses. The result of our analysis is that the lower limits on the masses of the scalar triplet fields are higher than that of the fermionic triplet fields.

Next, we have addressed on the implications of the constraints from LFV processes on observable quantities such as the anomalous magnetic moment of the muon, $(g - 2)_\mu$. In the case of degenerate mass pattern of neutrinos, the contribution to the $(g - 2)_\mu$ from the scalar and fermionic triplet Higgses can fit the current discrepancy in it. However, after applying the constraints from the above described LFV processes, this contribution would be at most 3.4×10^{-11} , which is two orders less than the required amount.

We have also studied on the detection of scalar triplet fields in a collider experiment, for which we have studied the decays of these fields under a simplified assumption of zero

mixing between the two hypercharged triplet scalar fields. The golden channel to detect a scalar triplet Higgs is $\phi_1^{++} \rightarrow \ell^+ \ell^+$, and we have addressed how this channel would be affected due to the presence of the decay modes involving supersymmetric particles. Our study suggests that the above mentioned golden channel may not compete against the decay modes into supersymmetric particles, however, for some suitable choice of model parameters we can still have significant branching ratio for $\phi_1^{++} \rightarrow \ell^+ \ell^+$. Similarly, the constraints from LFV and the choice of parametric space of the model give us indication about the dominant decay channels of singly charged (ϕ_1^+) and neutral (ϕ_1^0) scalar triplet Higgses.

Acknowledgments

The author is thankful to Dilip Kumar Ghosh for valuable discussions and also for reading the manuscript.

Appendix

A) Scalar potential

The scalar potential of the SUSY Type II seesaw model at TeV scale will have the following form.

$$\begin{aligned}
V &= \sum_Y \left| \frac{\partial W}{\partial Y} \right|^2 + \frac{1}{2} \sum_{a=1}^3 D^a D^a + \frac{1}{2} D^Y D^Y + V_{\text{soft}}^{\text{MSSM}} + V_{\text{soft}}^{\text{triplet}}, \\
D^a &= -g \left(H_d^\dagger \frac{\sigma^a}{2} H_d + H_u^\dagger \frac{\sigma^a}{2} H_u + \Phi_1^\dagger T^a \Phi_1 + \Phi_2^\dagger T^a \Phi_2 \right), \\
D^Y &= -\frac{g'}{2} \left(H_u^\dagger H_u - H_d^\dagger H_d \right) - g' \left(\Phi_1^\dagger \Phi_1 - \Phi_2^\dagger \Phi_2 \right).
\end{aligned} \tag{22}$$

The first term in Eq. (22) is the F -term contribution where the summation over the fields Y run over the superfields of W of Eq. (1). The second and third terms of Eq. (22) are D -term contributions due to $\text{SU}(2)_L$ and $\text{U}(1)_Y$ gauge groups, respectively. The last two terms of Eq. (22) are soft terms of MSSM and fields involving triplet scalar fields. The form of $V_{\text{soft}}^{\text{MSSM}}$ can be found in Ref. [6, 7]. The $V_{\text{soft}}^{\text{triplet}}$ is given in Eq. (5). The triplet

representation of SU(2) generators, which are needed in D^a of Eq. (22), are

$$T^1 = \frac{1}{\sqrt{2}} \begin{pmatrix} 0 & 1 & 0 \\ 1 & 0 & 1 \\ 0 & 1 & 0 \end{pmatrix}, \quad T^2 = \frac{1}{\sqrt{2}} \begin{pmatrix} 0 & -i & 0 \\ i & 0 & -i \\ 0 & i & 0 \end{pmatrix}, \quad T^3 = \begin{pmatrix} 1 & 0 & 0 \\ 0 & 0 & 0 \\ 0 & 0 & -1 \end{pmatrix}. \quad (23)$$

For computing D -terms, the forms of the scalar fields are as follows: $H_u = (H_u^+, H_u^0)^T$, $H_d = (H_d^0, H_d^-)^T$, $\Phi_1 = (\phi_1^{++}, \phi_1^+, \phi_1^0)^T$, $\Phi_2 = (\phi_2^0, \phi_2^-, \phi_2^{--})^T$. We have described the D -terms of doublet and triplet Higgses, but the D -terms for other fields of the model can be analogously written.

B) Conventions of neutralino and chargino mass matrices and their diagonalizing matrices

Our conventions regarding neutralino and chargino mass matrices are same as in [7]. In the basis $\Psi^0 = (\tilde{B}, \tilde{W}^3, \tilde{H}_d, \tilde{H}_u)^T$, the mixing mass matrix of neutralinos can be written as $\mathcal{L}_N = -\frac{1}{2} (\Psi^0)^T M_N \Psi^0 + \text{h.c.}$. The form of M_N is same as that of $\mathbf{M}_{\tilde{\mathbf{N}}}$ in Sec. 8.2 of Ref. [7]. The physical neutralino states are defined from $\Psi_j^0 = \sum_{k=1}^4 V_{jk}^N N_k$, where the unitary matrix V^N diagonalizes M_N as

$$(V^N)^T M_N V^N = \text{diag}(m_{N1}, m_{N2}, m_{N3}, m_{N4}). \quad (24)$$

In the basis: $\Psi^- = (\tilde{W}^-, \tilde{H}_d^-)^T$, $\Psi^+ = (\tilde{W}^+, \tilde{H}_u^+)^T$, the mixing mass terms for charginos can be written as $\mathcal{L}_c = -(\Psi^-)^T M_C \Psi^+ + \text{h.c.}$. The matrix M_C is same as that of \mathbf{X} in Sec. 8.2 of Ref. [7]. The physical chargino states are defined from: $\Psi_j^- = \sum_{k=1}^2 U_{jk}^\chi \chi_k^-$, $\Psi_j^+ = \sum_{k=1}^2 V_{jk}^\chi \chi_k^+$. The unitary matrices U^χ and V^χ diagonalize M_C as

$$(U^\chi)^T M_C V^\chi = \text{diag}(m_{C1}, m_{C2}). \quad (25)$$

References

- [1] G. Aad *et al.* [ATLAS Collaboration], Phys. Lett. B **716**, 1 (2012) [arXiv:1207.7214 [hep-ex]]; S. Chatrchyan *et al.* [CMS Collaboration], Phys. Lett. B **716**, 30 (2012) [arXiv:1207.7235 [hep-ex]].
- [2] M. E. Peskin, In *Carry-le-Rouet 1996, High-energy physics* 49-142 [hep-ph/9705479]; G. Altarelli, Nucl. Instrum. Meth. A **518**, 1 (2004)

- [hep-ph/0306055]; C. Quigg, hep-ph/0404228; J. Ellis, Nucl. Phys. A **827**, 187C (2009) [arXiv:0902.0357 [hep-ph]].
- [3] T. Mori, eConf C **060409**, 034 (2006) [hep-ex/0605116]; J. M. Yang, Int. J. Mod. Phys. A **23**, 3343 (2008) [arXiv:0801.0210 [hep-ph]]; A. J. Buras, Acta Phys. Polon. Supp. **3**, 7 (2010) [arXiv:0910.1481 [hep-ph]]; Y. Nir, CERN Yellow Report CERN-2010-001, 279-314 [arXiv:1010.2666 [hep-ph]].
- [4] For a review on neutrino masses and mixing, see R. N. Mohapatra, hep-ph/0211252; Y. Grossman, hep-ph/0305245; A. Strumia and F. Vissani, hep-ph/0606054.
- [5] M. Magg and C. Wetterich, Phys. Lett. B **94**, 61 (1980); R. N. Mohapatra and G. Senjanovic, Phys. Rev. **D23**, 165 (1981); G. Lazarides, Q. Shafi and C. Wetterich, Nucl. Phys. B **181**, 287 (1981).
- [6] H. P. Nilles, Phys. Rept. **110**, 1 (1984); H. E. Haber and G. L. Kane, Phys. Rept. **117**, 75 (1985); M. Drees, R. Godbole and P. Roy, Theory and Phenomenology of Sparticles, (World Scientific, 2004); P. Binetruy, Supersymmetry (Oxford University Press, 2006); H. Baer and X. Tata, Weak Scale Supersymmetry: From Superfields to Scattering Events, (Cambridge University Press, 2006).
- [7] S. P. Martin, arXiv:hep-ph/9709356.
- [8] T. Hambye, E. Ma and U. Sarkar, Nucl. Phys. B **602**, 23 (2001) [hep-ph/0011192]; A. Rossi, Phys. Rev. D **66**, 075003 (2002) [hep-ph/0207006].
- [9] M. Hirsch, S. Kaneko and W. Porod, Phys. Rev. D **78**, 093004 (2008) [arXiv:0806.3361 [hep-ph]]; J. N. Esteves, J. C. Romao, A. Villanova del Moral, M. Hirsch, J. W. F. Valle and W. Porod, JHEP **0905**, 003 (2009) [arXiv:0903.1408 [hep-ph]].
- [10] See Ref. [8](a); S. Antusch and S. F. King, Phys. Lett. B **597**, 199 (2004) [hep-ph/0405093]; E. J. Chun and S. Scopel, Phys. Lett. B **636**, 278 (2006) [hep-ph/0510170]; M. Senami and K. Yamamoto, Int. J. Mod. Phys. A **21**, 1291 (2006) [hep-ph/0305202].
- [11] A. G. Akeroyd and S. Moretti, Phys. Rev. D **86**, 035015 (2012) [arXiv:1206.0535 [hep-ph]].
- [12] D. K. Ghosh, R. S. Hundi and I. Saha, *in preparation*.

- [13] J. Beringer *et al.* (Particle Data Group), Phys. Rev. D **86**, 010001 (2012).
- [14] E. J. Chun, K. Y. Lee and S. C. Park, Phys. Lett. B **566**, 142 (2003) [hep-ph/0304069]; M. Kakizaki, Y. Ogura and F. Shima, Phys. Lett. B **566**, 210 (2003) [hep-ph/0304254]; E. K. Akhmedov and W. Rodejohann, JHEP **0806**, 106 (2008) [arXiv:0803.2417 [hep-ph]]; W. Rodejohann, Pramana **72**, 217 (2009) [arXiv:0804.3925 [hep-ph]].
- [15] A. G. Akeroyd, M. Aoki and H. Sugiyama, Phys. Rev. D **79**, 113010 (2009) [arXiv:0904.3640 [hep-ph]].
- [16] T. Fukuyama, H. Sugiyama and K. Tsumura, JHEP **1003**, 044 (2010) [arXiv:0909.4943 [hep-ph]].
- [17] M. Senami and K. Yamamoto, Phys. Rev. D **69**, 035004 (2004) [hep-ph/0305203].
- [18] For a review on the muon ($g - 2$), see, Z. Zhang, arXiv:0801.4905 [hep-ph]; F. Jegerlehner and A. Nyffeler, Phys. Rept. **477**, 1 (2009) [arXiv:0902.3360 [hep-ph]].
- [19] R. S. Hundi, S. Pakvasa and X. Tata, Phys. Rev. D **79**, 095011 (2009) [arXiv:0903.1631 [hep-ph]].
- [20] J. Adam *et al.* [MEG Collaboration], Phys. Rev. Lett. **107**, 171801 (2011) [arXiv:1107.5547 [hep-ex]].
- [21] J. Chakraborty, P. Ghosh and W. Rodejohann, arXiv:1204.1000 [hep-ph].
- [22] Y. Abe *et al.* [DOUBLE-CHOOZ Collaboration], Phys. Rev. Lett. **108**, 131801 (2012) [arXiv:1112.6353 [hep-ex]]; F. P. An *et al.* [DAYA-BAY Collaboration], Phys. Rev. Lett. **108**, 171803 (2012) [arXiv:1203.1669 [hep-ex]]; J. K. Ahn *et al.* [RENO Collaboration], Phys. Rev. Lett. **108**, 191802 (2012) [arXiv:1204.0626 [hep-ex]].
- [23] S. Chatrchyan *et al.* [CMS Collaboration], arXiv:1207.2666 [hep-ex].
- [24] D. V. Forero, M. Tortola and J. W. F. Valle, arXiv:1205.4018 [hep-ph].
- [25] P. F. Harrison, D. H. Perkins and W. G. Scott, Phys. Lett. B **530**, 167 (2002) [hep-ph/0202074].

- [26] T. Moroi, Phys. Rev. D **53**, 6565 (1996) [Erratum-ibid. D **56**, 4424 (1997)] [hep-ph/9512396]; S. P. Martin and J. D. Wells, Phys. Rev. D **64**, 035003 (2001) [hep-ph/0103067].
- [27] R. S. Hundi, Phys. Rev. D **83**, 115019 (2011) [arXiv:1101.2810 [hep-ph]].
- [28] J. F. Gunion, R. Vega and J. Wudka, Phys. Rev. D **42**, 1673 (1990); R. Godbole, B. Mukhopadhyaya and M. Nowakowski, Phys. Lett. B **352**, 388 (1995) [hep-ph/9411324]; K. -m. Cheung, R. J. N. Phillips and A. Pilaftsis, Phys. Rev. D **51**, 4731 (1995) [hep-ph/9411333]; M. Muhlleitner and M. Spira, Phys. Rev. D **68**, 117701 (2003) [hep-ph/0305288]; A. G. Akeroyd and M. Aoki, Phys. Rev. D **72**, 035011 (2005) [hep-ph/0506176]; T. Han, B. Mukhopadhyaya, Z. Si and K. Wang, Phys. Rev. D **76**, 075013 (2007) [arXiv:0706.0441 [hep-ph]].
- [29] D. A. Demir, M. Frank, D. K. Ghosh, K. Huitu, S. K. Rai and I. Turan, Phys. Rev. D **79**, 095006 (2009) [arXiv:0903.3955 [hep-ph]].
- [30] A. G. Akeroyd and H. Sugiyama, Phys. Rev. D **84**, 035010 (2011) [arXiv:1105.2209 [hep-ph]].
- [31] N. Arkani-Hamed, A. G. Cohen, E. Katz and A. E. Nelson, JHEP **0207**, 034 (2002) [hep-ph/0206021].
- [32] T. Han, H. E. Logan, B. Mukhopadhyaya and R. Srikanth, Phys. Rev. D **72**, 053007 (2005) [hep-ph/0505260].